Supporting Information

Microfluidic-based assessment of cell deformability

Andrea Adamo,[a] Armon Sharei,[a] Luigi Adamo,[b] ByungKun Lee,[c] Shirley Mao [a] and Klavs F. Jensen[a1]

[a]Department of Chemical Engineering, MIT, 77 Massachusetts Avenue, Cambridge, MA 02139, USA,

[b]Department of Medicine, Washington University School of Medicine St Louis, 660 S. Euclid Ave., St. Louis, MO 63110

[c]Department of Electrical Engineering and Computer Science, MIT, 77 Massachusetts Avenue, Cambridge, MA 02139, USA.

Sensing area electrical model.

The model of Foster and Schwan[1] is usually used for the analysis of the electrical behavior of a cell in a suspension. In this model, the cell is approximated as a resistor, R_i, describing the cytoplasm, in series with a capacitor, C_{mem}, representing the cell membrane. To complete the model, the electrical equivalent of the cell is in parallel with the medium resistance, R_m, and medium capacitance, C_m. In order to include the interface between the electrodes and the

[1] Corresponding author kfjensen@mit.edu

suspension medium, the capacitance of the electric double layer, C_{DL}, also needs to be added (Fig S1).

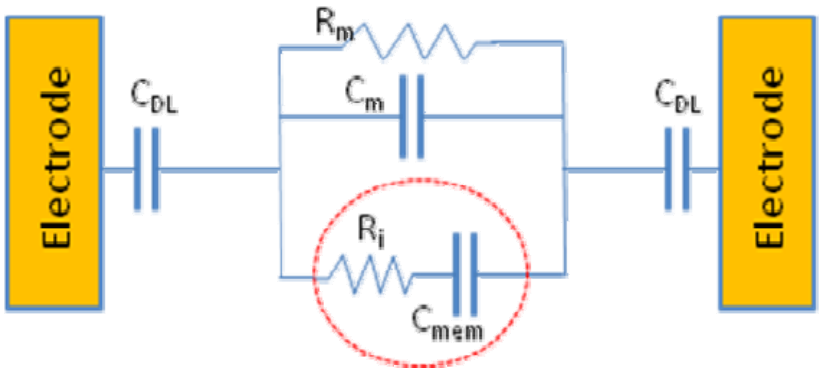

Figure S1: Electrical scheme of the sensing area with a cell between the electrodes. The cell is represented as a resistor, R_i, describing the cytoplasm, and a capacitor C_{mem}, representing the cell membrane. The liquid medium is represented by a resistance, R_m, and medium capacitance, C_m. C_{DL}, is the capacitance of the electric double layers at the interfaces between the electrodes and the medium.

According to the above mentioned model, the values of the elements of the circuit are given by[1b]:

$$R_m = \frac{1}{\sigma_m\left(1-\frac{3\Phi}{2}\right)G_f} \tag{1}$$

$$C_m = \varepsilon_\infty G_f \tag{2}$$

$$C_{mem} = \frac{9}{4}\Phi R C_{mem,0} G_f \tag{3}$$

$$R_i = \frac{4\left(\frac{1}{2\sigma_m}+\frac{1}{\sigma_i}\right)}{9\Phi G_f} \tag{4}$$

Here σ_m is the medium conductivity, Φ is the volume fraction occupied by the cell, $C_{mem,0}$ is the cell membrane capacitance per unit area, and R is the cell radius. G_f depends on the geometry and for an ideal parallel plate electrode system, which can be assumed in the present case, it is the ratio of electrode area to electrode distance. σ_i is the cytoplasm conductivity. The limiting

high frequency permittivity of the suspension, ε_∞, is related to the suspending medium permittivity by:

$$\varepsilon_\infty = \varepsilon_m \left[1 - 3\Phi \frac{\varepsilon_m - \varepsilon_i}{2\varepsilon_m + \varepsilon_i} \right] \quad (5)$$

Where ε_m and ε_i are the permittivity of the medium and the cell interior, respectively. The impedance of the cell suspension Z_s (without the double layer capacitance) is given by:

$$Z_s = \left[\frac{1}{R_m} + j\omega C_m + \frac{1}{R_i + \frac{1}{j\omega C_{mem}}} \right] \quad (6)$$

with $j = \sqrt{-1}$ and ω the angular frequency.

Figure S2 shows the impedance change with frequency for different cell sizes, including the no cell case (Φ=0). The values selected for the parameters required for the plot are taken from literature (see caption for details), the volume fraction is calculated on the actual dimension of the device. G_f is approximated as the value for a uniform field between parallel plates based on the geometry (the distance between the electrodes is much larger than the channel height and width). Differences in G_f from the parallel plates case would alter the numerical values of the graph but would not change the general behavior of the impedance as a function of frequency, $Z_s(\omega)$.

The model shows the Maxwell–Wagner dispersion around 0.6-1.1 MHz and the beginning of the capacity behavior of the detection volume around 30 Mhz. For frequencies below the Maxwell-Wagner dispersion, the cell can often be regarded as an insulator and sizing can then be accomplished in line with previous studies.[2, 3, 4, 5]

The impedance contribution of the double layer Z_{DL} cannot be neglected in the measurement. The modulus of the total impedance Z between the electrodes ($Z = Z_S + Z_{DL}$) significantly increases, but at a set frequency $\Delta Z/Z$ still depends on the volume of the cell (Figure S3). Working at frequencies around 100kHz (lower than the Maxwell-Wagner dispersion) would provide a measurement with good sensitivity because the role of the double layer capacitance becomes negligible and cell size information is retained.

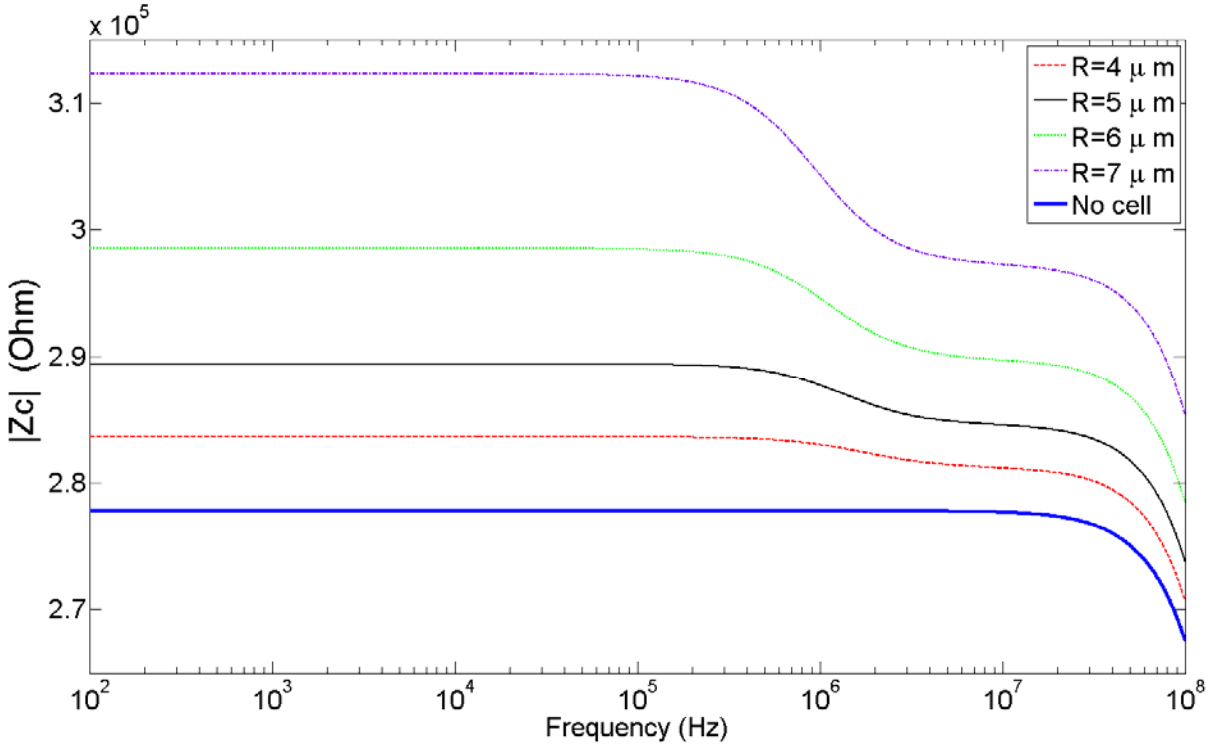

Figure S2: Impedance as a function of frequency for different cell diameters including the no cell case. The plot is based on the following parameters[18] σ_m=1.6 S/m; σ_i=0.5S/m; $C_{mem,0}$=1μF/cm^2; ε_m=80 ε_0, ε_i=60 ε_0 ; ε_0=8.854$\times$ 10^{-12} F/m. The cell fraction is computed for each cell radius with the actual volume of the sensing area (1.95 pl).

The present device was fabricated in silicon as it provided the advantage of established techniques for the fabrication of the small funnel shape in the channel with tight tolerances, but its electrical properties forced us to run the circuitry at frequencies below 100 KHz to minimize the influence of the silicon. We ran experiments at 20 KHz as a compromise among time resolution, limited loss in the silicon and reasonable impedance increase due to the double layer capacitance. At 20kHz a cell of radius 4 micron would theoretically give an impedance change of about 1% whereas a cell with radius of 7 micron would give a variation of about 5% (Figure 5 insert). As expected from the Foster –Schwartz theory, the impedance variation scales linearly with the cell volume.

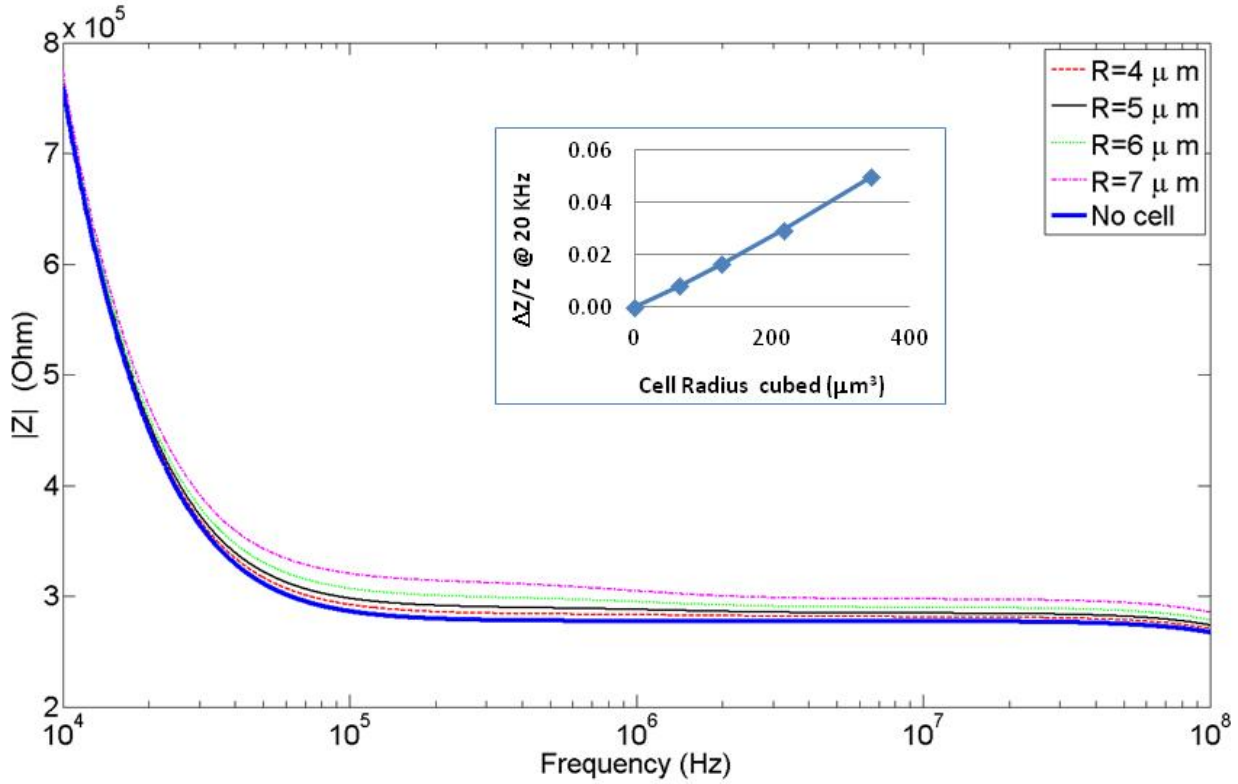

Figure S3: a) Modulus of the impedance $Z=Z_S+Z_{DL}$ The Capacitance of the double layer used for the simulation is 15μF/cm^2 (see ref [19]). Other values as in the model of Z_S and figure S2. b) ΔZ/Z at 20 KHz as a function of cell radius cubed (the plotted points correspond to radii R = 0, 4, 5, 6, 7 μm).

Results of experiments on human primary fibroblasts:

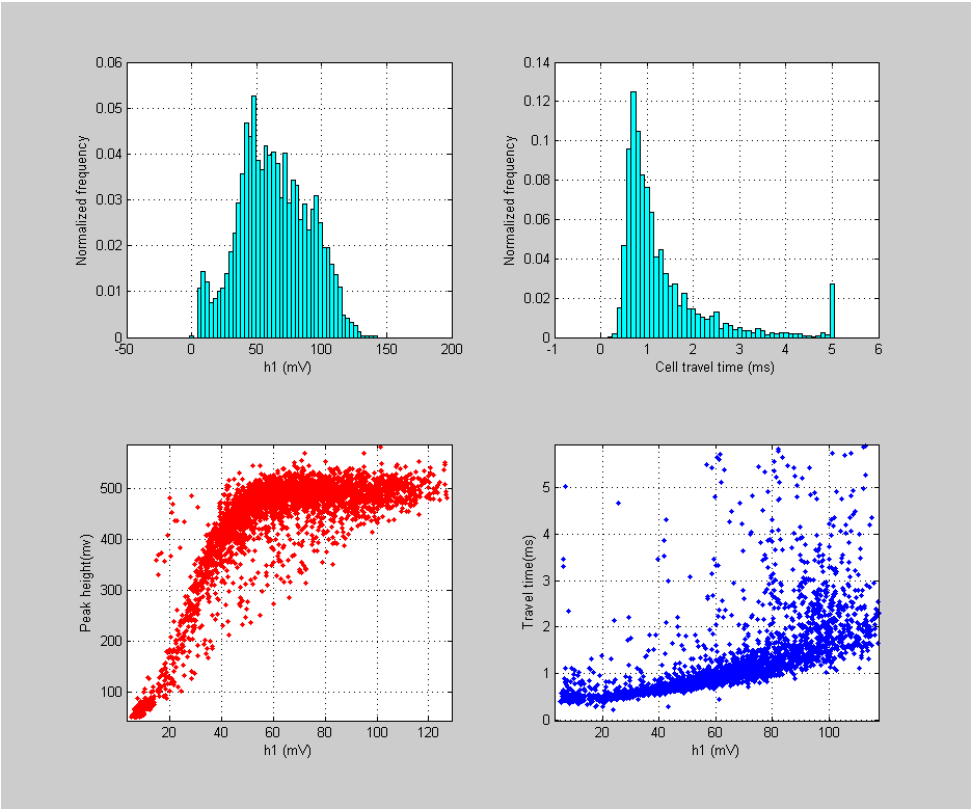

Figure S4: Human primary fibroblasts are flown through the device with a flow pressure of 4 psi. a) Histogram of the value of the flat area of the signal h1. h1 appears to have a symmetric bell shaped distribution as expected for a measurement of cell size in cultured cells. The bar at 0 mv represents the fraction of cells for which the code did not succeed to retrieve h1. B) Histogram of cell travel time through the funnel shaped constriction. Travel time has a non-symmetric distribution with a long tail at higher transversal times side. The bar at 2ms represents all the cells with travel time higher than 2 ms. C) Relationship between peak height h2 and value of flat area h1. h2 (maximum resistance observed at the passage of the cell) depends linearly on h1 (cell size) for low values of h1 but saturates around h1=~50mV. D) Relationship between cell travel time Δt and value of flat area h1. The scattering of travel time values increases for values of h1 larger than ~50mV.

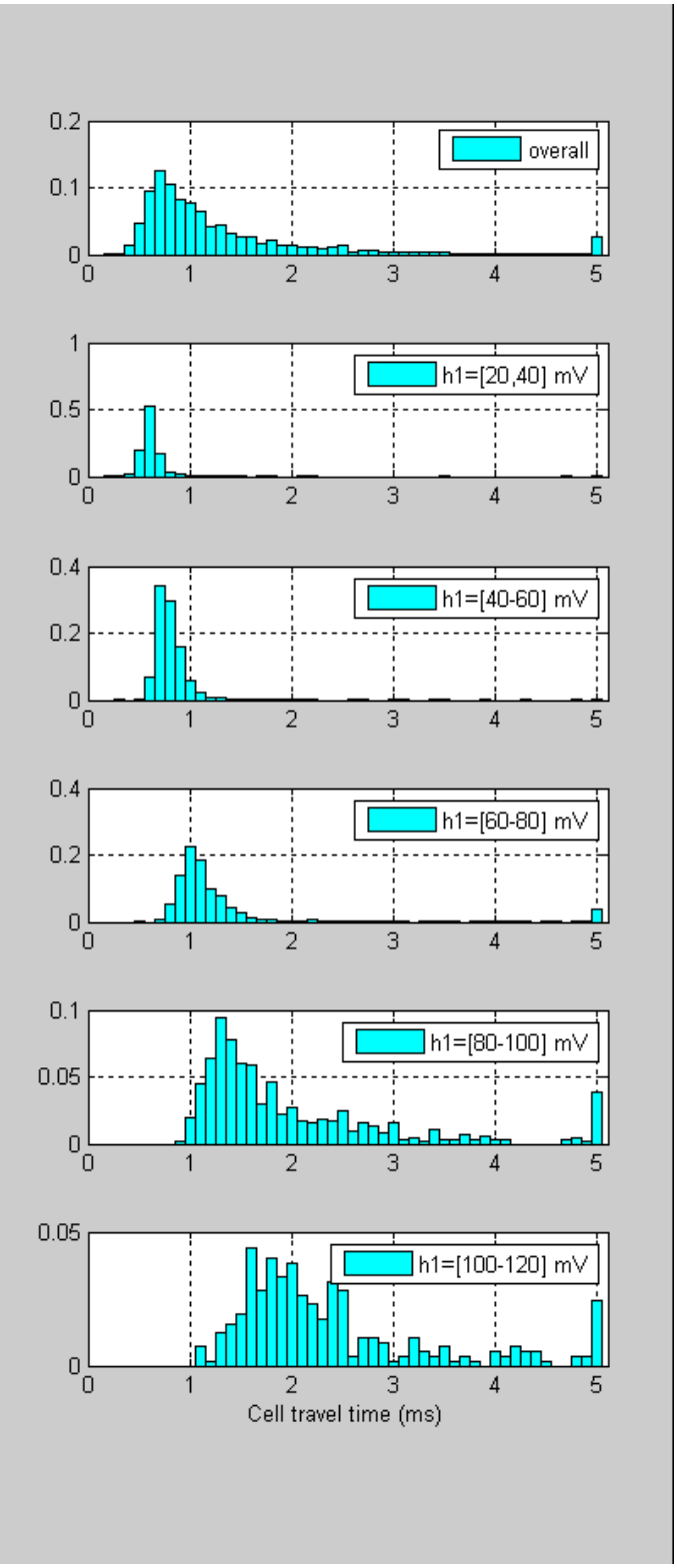

Figure S5: Cell travel time through the microchannel narrowing depends on cell diameter**.** Top graph - Histogram of cell transit time measured on human primary fibroblasts. Transit time has a non symmetric, wide distribution. Cell transit time is significantly influenced by diameter with larger cells showing longer transit times than smaller cells. All cells with travel time > 2ms are pooled in the 2ms bar.

Results of experiments on HeLa cells with Cythocalasin B

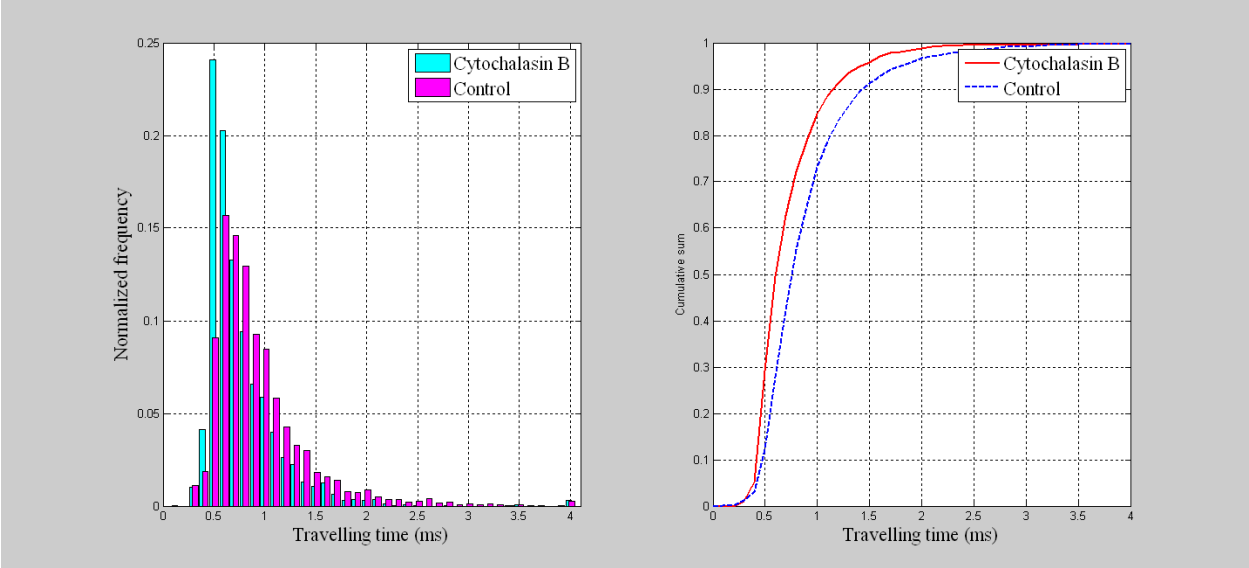

Figure S6: Cell travel time through the microchannel narrowing depends on cell deformability. HeLa cells were treated with Cytochalasin B (20 μM for 30 min) to interfere with actin polymerization and reduce cell stiffness. Left: Histogram of the travel time of treated sample and the control (samples are taken from the same original population and flown on the same chip). Right: cumulative sums of the travel time histograms for both treated and control sample. The travel time of the treated sample is shorter than the control for any percentile.

References:

1. (a) K. R. Foster, H. P. Schwan, *Crit Rev Biomed Eng* **1989**, *17*. 25; (b) T. Sun, H. Morgan, *Microfluidics and Nanofluidics* **2010**, *8*. 423.
2. S. Gawad, L. Schild, P. H. Renaud, *Lab Chip* **2001**, *1*. 76.
3. S. Gawad, K. Cheung, U. Seger, A. Bertsch, P. Renaud, *Lab Chip* **2004**, *4*. 241.
4. D. Malleo, J. T. Nevill, L. P. Lee, H. Morgan, *Microfluid Nanofluidics* **2010**, *9*. 191.
5. A. Valero, T. Braschler, P. Renaud, *Lab Chip* **2010**, *10*. 2216.